Treatment Of Surface Bidirectional Reflectance And Albedo In The ORAC-(A)ATSR Aerosol Retrieval

A. M. Sayer, G. E. Thomas, R. G. Grainger

Atmospheric, Oceanic and Planetary Physics, Department of Physics, University of Oxford

sayer@atm.ox.ac.uk

Introduction

Particularly over the land and the sun-glint region of the sea, a large proportion of the top-of-atmosphere (TOA) radiance measured by a satellite radiometer in the visible and near-infrared arises from the reflection of incident solar radiation off the Earth's surface. Knowledge of the surface bidirectional reflectance distribution function (BRDF) is therefore important to partition accurately the contributions from the atmosphere and surface to the measurements. This poster presents a summary of the treatment of the BRDF in the Oxford-RAL Aerosol and Cloud (ORAC) scheme, as applied to the (A)ATSR instruments. To model surface-atmosphere interactions, three types of reflectance must be defined:

1. The BRDF, R_{bb}. This represents direct reflectance of direct radiation, and the models used are described in this poster.
2. The black-sky albedo, R_{bd}. This represents diffuse reflectance of direct radiation and is obtained by integrating the BRDF over all satellite zenith and relative azimuth angles.
3. The white-sky albedo, R_{dd}. This represents diffuse reflectance of diffuse radiation and is obtained by integrating the black-sky albedo over all solar zenith angles.

The white-sky albedo is reported as the retrieved quantity at each wavelength used (550 nm, 670 nm, 870 nm, 1,6 µm). The ratios R_{bb}:R_{dd} and R_{bd}:R_{dd} are fixed by the BRDF model used for each pixel, and the three types of reflectance scaled in the retrieval.

Sea Surface Reflectance

Over sea, a model has been developed based on the method of Koepke (1984), which includes contributions from oceanic whitecaps, specular reflectance from the ocean surface ('Sun-glint'), and upwelling radiance from under the surface ('underlight').

Whitecaps

Wind blowing across the sea surface generates patches of bright whitecaps; these can significantly enhance the BRDF in water away from the Sun-glint region. Whitecap coverage is parameterised using wind data from ECMWF and the method of Monahan & Muircheartaigh (1980). To the right is the fractional whitecap coverage (black dashed) and the whitecap contribution to the surface reflectance, assumed isotropic, at 550 nm and 670 nm (red), 870 nm (blue), and 1.6 µm (green) as a function of wind speed. Typical wind speeds are in the range 3-15 ms^{-1}.

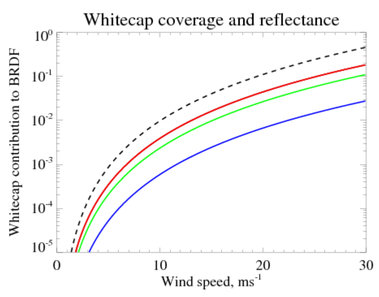

Sun-Glint

The glint contribution is determined according to Cox & Munk (1954*a*,*b*), using ECMWF wind data. Traditionally, the region of an orbit affected by strong Sun-glint is omitted from satellite aerosol retrievals due to the bright surface. However, this BRDF model, combined with the dual-viewing geometry of the ATSR instruments, allows continuous retrieval into this Sun-glint region. Glint reflectance is of similar magnitude at all wavelengths. The figure to the right shows the glint contribution at 550 nm as a function of solar zenith and relative azimuth angles, for a wind speed of 5 ms^{-1} and relative wind azimuth of 135º for instrument zenith angles of 5º (top) and 55º (bottom).

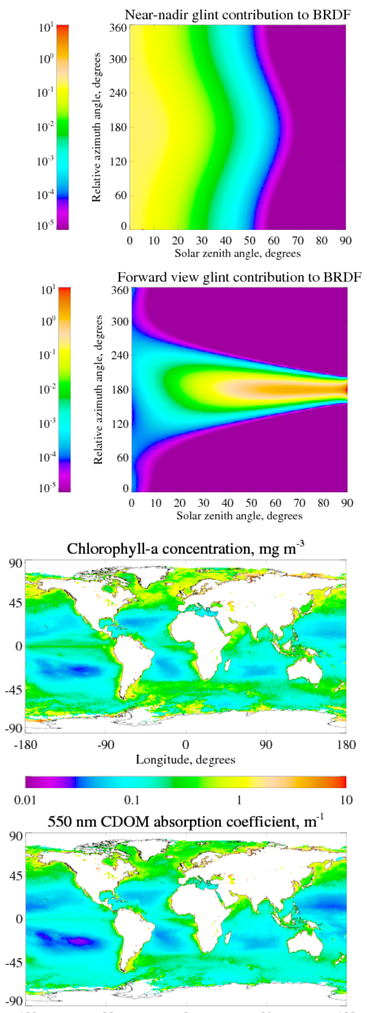

Underlight

Scattering from dissolved organic matter and water molecules give rise to an `underlight' contribution to the BRDF. This is based on the method of Morel (1988) for Case I waters, and uses chlorophyll-*a* and coloured dissolved organic matter (CDOM) data from the GlobColour project. The annual mean chlorophyll-*a* concentration and CDOM absorption coefficient for the year 2004 are shown to the right. Underlight has small geometric dependence and the magnitude of the contribution decreases rapidly with increasing wavelength.

Typical Values

An example swath over the Atlantic from September 2004 is shown to the right. All figures use the same scale to emphasise the comparative variability; results at 550 nm (where all contributions are significant) and 1.6 µm (dominated by glint) are shown. The BRDF may vary over several orders of magnitude; conversely, R_{dd} is typically 0.04-0.08, dependent on wavelength.

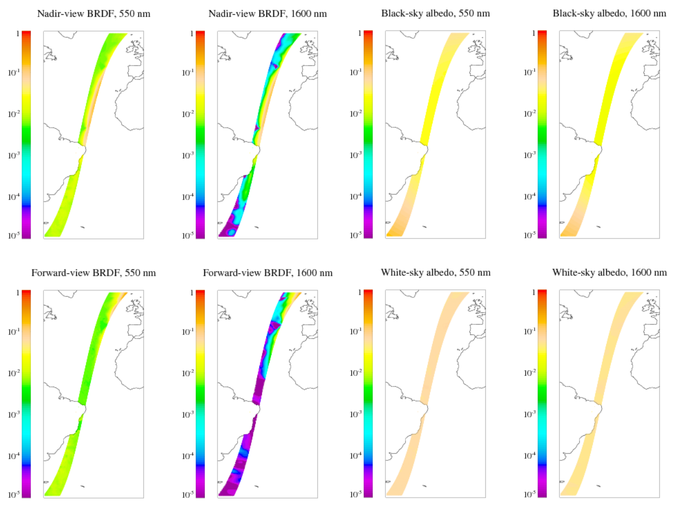

Land Surface Reflectance

Over land, the 8-day MODIS BRDF model parameter product (MCD43B1; Wanner *et al*, 1995, 1997) is used. Together with the Ambrals forward model, this defines the BRDF for a viewing geometry as a weighted combination of reflectance from three kernels. These kernels represent isotropic, geometric and volumetric scattering from different types of surface.

Sensor Differences

AATSR and MODIS are different sensors. As their spectral response functions (right, with AATSR in black and MODIS in red) do not match, they will report a different albedo for the same underlying surface. A technique is presented to quantify this source of error and correct for it.

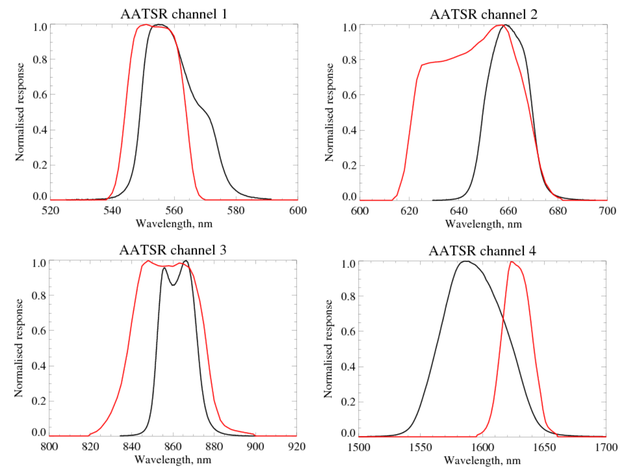

Quantification Of Potential Error

Convolving the instrument response functions with 151 high-resolution spectra from the ASTER and USGS libraries for a variety of surface types creates a dataset of the effective albedo each instrument would see for that surface. This reveals that the impact of the sensor differences can be large, with clear biases dependent on surface type. To the right is the difference (MODIS-AATSR 'observed' albedo) as a function of the AATSR albedo, for vegetation spectra (green stars), sand (red triangles), soil (orange squares), snow and ice (blue diamonds) and man-made surfaces (black crosses).

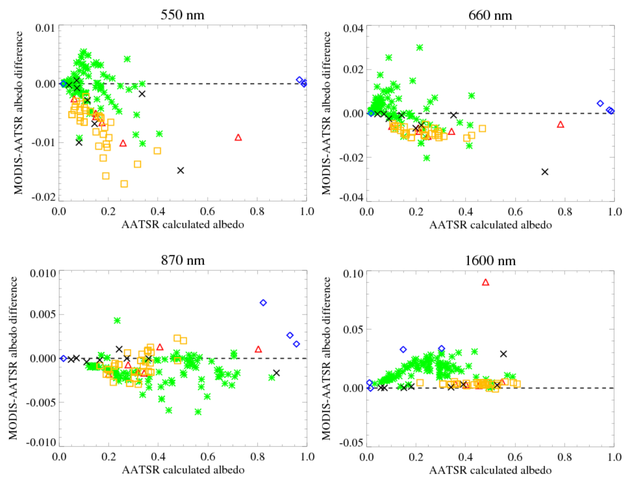

SVD-Based Correction

The technique of singular value decomposition (SVD) can be used with this 151-spectra dataset to obtain singular vectors describing the variability of albedo for both instruments. Fitting MODIS albedo at 4 wavelengths to these vectors gives coefficients to reconstruct what the AATSR albedo would be. This results in an improved (by generally ~60%) estimate of the AATSR albedo as compared to using the MODIS albedo alone, as shown to the right (same key as before). The biases are noticeably reduced. Use of the extra MODIS bands near 440 nm, 1.2 µm and 2.2 µm provides little further improvement.

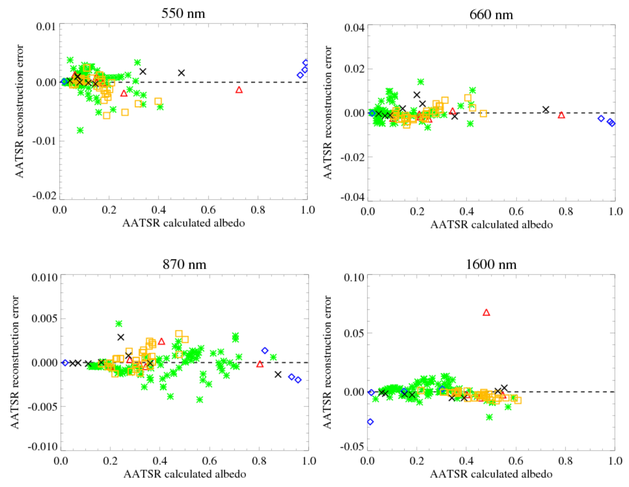

Example Application

Operationally, the MODIS data product is used to generate $R_{bb,M}$, $R_{bd,M}$ and $R_{dd,M}$ for each pixel (where M denotes a MODIS-like sensor). The SVD technique is then used to correct these reflectances for each wavelength to account for sensor differences. The resulting data are then used to initialise the retrieval. The correction made to the white-sky albedo is shown to the right for an example swath over Europe; these adjustments are consistent with the expected differences shown above.

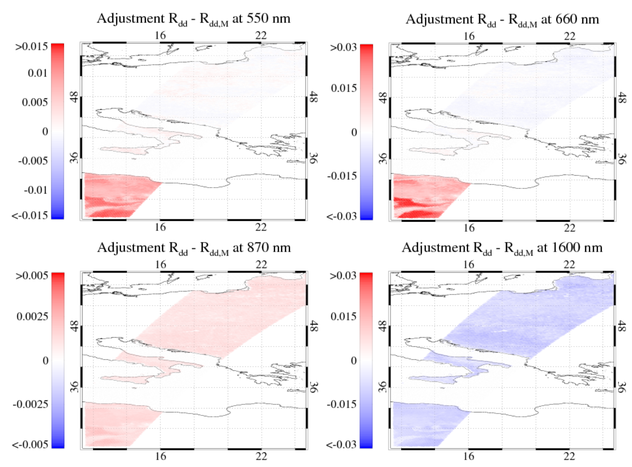

Key References: Sea

- Cox & Munk, *J. Opt. Soc. Am.*, 44 (1954*a*), doi:10.1364/JOSA.44.000838
- Cox & Munk, *J. Mar. Res.*, 13 (1954*b*)
- Koepke, *Appl. Opt.*, 23 (1984), doi:10.1364/AO.23.001816
- Monahan & Muircheartaigh, *J. Phys. Oceaonogr.*, 10 (1980).
- Morel, *J. Geophys. Res.*, 93 (1988)
- GlobColour project website: *http://www.globcolour.info/*

Acknowledgements

ESA and the NEODC are thanked for provision of the AATSR and GlobColour data. ECMWF are thanked for the wind data used. NASA and BU are thanked for the MODIS BRDF parameter dataset, and many useful discussions about it. This work was supported by the NERC National Centre for Earth Observation.

Key References: Land

- Wanner *et al.*, *J. Geophys. Res.*, 100 (1995), doi:10.1029/95JD02371.
- Wanner *et al.*, *J. Geophys. Res.*, 102 (1997), doi:10.1029/96JD03295
- ASTER spectral library: *http://speclib.jpl.nasa.gov/*
- USGS spectral library splib05a: *http://pubs.usgs.gov/of/2003/ofr-03-395/*